CIRCUM-PROTOSTELLAR ENVIRONMENTS II. ENVELOPES, ACTIVITY, AND EVOLUTION

G.H. Moriarty-Schieven[1], P. G. Wannier[2]
Jocelyn Keene[3], M. Tamura[4]

[1]Dominion Radio Astrophysical Observatory, National Research Council, Box 248, Penticton, British Columbia, V2A 6K3, Canada

[2]Jet Propulsion Laboratory, MS 169-506, 4800 Oak Grove Dr., Pasadena, CA 91109

[3]Caltech Submillimeter Observatory, Division of Physics, Mathematics and Astronomy, California Institute of Technology, MS 320-47, Pasadena, CA 91125

[4]National Astronomical Observatory, Osawa 2-21-1, Mitaka, Tokyo 181, Japan

Submitted to The Astrophysical Journal.

CIRCUM-PROTOSTELLAR ENVIRONMENTS II. ENVELOPES, ACTIVITY, AND EVOLUTION

G. H. Moriarty-Schieven
Dominion Radio Astrophysical Observatory, National Research Council, Box 248, Penticton, British Columbia, V2A 6K3, Canada

P. G. Wannier
Jet Propulsion Laboratory, MS 169-506, 4800 Oak Grove Dr., Pasadena, CA 91109

Jocelyn Keene
Caltech Submillimeter Observatory, Division of Physics, Mathematics and Astronomy, California Institute of Technology, MS 320-47, Pasadena, CA 9112.5

and

M. Tamura
National Astronomical Observatory, Osawa 2-21-1, Mitaka, Tokyo 181, Japan

submitted to The Astrophysical Journal

ABSTRACT

We have obtained 800 and 1100 μm photometric observations of a complete, flux-limited, IRAS-selected sample of cold sources in Taurus, whose infrared and molecular properties indicate them to be low-mass protostars which are younger than T Tauri stars. The goal of this study is to understand the role of the circumstellar envelope and disk during low-mass star formation, and to search for signs of evolution. We find a good correlation between the sub-millimeter flux density (as well as of envelope mass) with both the mechanical luminosity of the molecular outflow and with the far-infrared luminosity, presumably produced by accretion onto the protostar. This suggests that the mass of the disk/envelope may be linked to the rate of accretion onto the protostar and to the generation of outflows. However, in contrast to the results of Cabrit & André, we see no evidence for a lower limit to the clisli/envelope mass which can produce outflows. We also find a significant difference between the spectral energy distributions (SEDs) at sub-millimeter wavelengths of embedded protostars compared to optically visible T Tauri stars. The more evolved (1' Tauri) objects tent] to have shallower spectral indices than embedded sources, suggesting (a) an evolution of dust grains, and/or (b) a more compact envelope and optically thick disk in the older objects.

Subject headings: stars: pre-main-sequence -- stars: formation -- Infrared: Interstellar: Continuum -- ISM: Jets and Outflows -- Stars: Circumstellar Matter

1. INTRODUCTION

The dense circumstellar environment, including the circumstellar disk and the cocooning envelope, plays a crucial role in the evolution of protostars. The circumstellar disk is believed: (a) to actively accrete onto the protostar, (b) to drive directly or indirectly the bipolar outflow, and (c) to be the likely site of planet formation. The surrounding envelope in turn is believed to accrete onto the circumstellar disk, and in early stages of star formation, directly onto the protostar itself (Shu, Adams & Lizano 1987).

The role played by the clisk/envelope in accretion and outflow is not well understood. Nevertheless this role is thought to be significant. Most of the luminosity of the protostar is believed to be derived from accretion (Shu, Adams & Lizano 1'387), and a significant fraction of the mass of the protostar may be accreted from the circumstellar disk (Hartmann & Kenyon 1985). outflows also have an obvious tie to the circumstellar environment. The bipolarity of the molecular outflow suggests an influence of a disk on the collimation of the winds, and the gravitational potential energy of the disk is the most likely source of outflow energy.

There is little direct evidence that the properties of the circumstellar environment influence accretion and outflow activity. Cabrit and André (1991) suggested that a minimum disk mass is required to generate an outflow, but Beckwith et al. (1990) found only a weak correlation between disk mass and accretion. Cabrit and Bertout (1992) have found the most convincing evidence to date of the correlation of molecular and ionized outflows with the bolometric luminosity of the protostar, but this still tells us little of the direct role of the disk/envelope, if any.

2. SOURCE SELECTION

We have chosen for our study a complete sample of cold, IRAS-selected objects in Taurus, whose far-infrared and molecular properties indicate them to be younger than T Tauri stars (Tamura et al., 1991; Moriarty -Schieven et al., 1992, hereafter Paper I). The positions used ("l'able 1) are those derived from their 2pm peak positions (Tamura et al. 1991; Draper et al. 1985), except for 04303 +2557, which has no compact $2\mu m$ counterpart. For this source, we made a small, irregularly-spaced map at $800\mu m$, and found the peak to be approximately 7" east, and 5" north of the IRAS position. Photometric observations were then made at this new position (listed in Table 1).

The source-selection criteria were as follows (Tamura et al 1991): (1) The sources are situated within a region covering a significant portion of the Taurus cloud complex; (2) The source colour is $log[F_{25\mu m}/F_{60\mu m}] <$ –0.25, i.e. they are cooler than T Tauri stars (Tamura & Sato 198'3); (3) The source flux density at 60 or $100\mu m$ is greater than 5 Jy, and IRAS flux densities are reliable (i.e. good flux qualities) at 25 through $100\mu m$; (4) Sources identified with galaxies or SAO stars are rejected. These criteria yielded 24 sources, and a further source (which dots not appear in the IRAS Point Source Catalogue), 1,1551 NE, was added since I ItAS-derived fluxes were available (Emerson et al. 1984) and it satisfies all other criteria.

Several lines of argument support their identification as protostar candidates. (1) The broad-band spectra] energy distribution of the sources is well reproduced by theoretical models of accreting protostars (Adams, Lada, and Shu 1987). (2) The age of tile sources is estimated to be $< 2 \times 10^5$ yr (younger than that Of T Tauri stars) from source number statistics, from source - cloud core separation, and from a comparison of an 11 R diagram based on 1 RAS colour and luminosity with theoretical protostar tracks (Beichman et al. 1986, Myers et al. 1987), (3) Many of the sources possess near-infrared reflection nebulae, suggestive of an

association with a molecular outflow cavity (Tamura et al. 1991), and this suspicion was confirmed when 3/4 of the sources were found to posess molecular outflows wit h dynamical lifetimes of< 0.1 – 2 x 10^5 years (Paper 1)[1]. The molecular outflow phase is believed to represent an earlier stage of evolution than that of T Tauri stars.

3. OBSERVATIONS

The sub-millimeterwave continuum observations presented in this paper were obtained from 8 to 12 September 1991, at the James Clerk Maxwell Telescope (JCMT[2]) on Mauna Kea, using the UKT14 continuum bolometer (Duncan et al. 1990). The telescope was equipped with a chopping secondary mirror, set to chop in azimuth by 60" at a frequency of 7.8 Hz. All photometry was obtained using the 65mm aperture. The filters used were 1100pm (center frequency 264 GHz (1090μm), bandwidth 75 GHz, half-power beamwidth (HPBW)$\sim$ 18.5"), and 800μm (center frequency 394 GHz (790μm), bandwidth 103 GHz, HPBW $\sim$ 16.8") (values from Matthews 1993). The source CRL618 was observed every 40-70 minutes throughout each night, in order to check the focus and pointing, and to derive atmospheric opacities at 800 and 1100μm. Pointing errors were $\lesssim$ 3" except at sunrise when the error could be as much as $\sim$ 4.5". (Except for L1551/IRS5, the positions of the sources were offset "blind" from CRL618, which is < 20° from most of the sources.) Through each night, the atmospheric opacity at 225 GHz (1300pm) was also monitored using the 225 GHz radiometer operated by the nearby Caltech Submillimeter Observatory. The opacity at 225 GHz was found to be very stable or only slowly varying over each night, with values of optical depth at 225 GHz ranging during the entire run from 0.10 to 0.14. Values derived from our JCMT observations of CRL618 were consistent with these. Primary flux calibration was done each night from observations of Mars, which was assumed to have a brightness temperature of 206K (yielding a flux density in the 65mm aperture of 110.4 J y/beam at 1100μm and 213.7 Jy/beam at 800μm).

Single point photometric observations at 800 and 1100μm were obtained toward most of the sources. (Flux densities for the remaining sources were obtained from the literature (see 'l'able 1).) The data were calibrated by correcting for atmospheric opacity, derived from our observations ofCR,LG18, and by converting to Jy/beam (assuming a sensitivity of 12.4 $\pm$ 0.4 Jy/mV at 1100μm and 9.9 $\pm$ 0.7 Jy/mV, found from our observations of Mars). The derived flux densities are presented in Table 1. The dominant source of error (shown in Table 1) is the uncertainty of calibration (contributing $\sim$7% uncertainty at 1100μm and $\sim$10% uncertainty at 800μm), caused mainly by variability of the sky opacity. Detections at the telescope were, however, at least 10σ. Only two sources were not detected at 800μm, and four were undetected at 1100μm. Quoted errors are 1σ, except for undetected sources where the 3σ upper limits are given.

At these wavelengths, the emission probes the warm dust in the circumstellar environment. It is reasonable to ask what fraction of the emission is coming from the circumstellar disk and what from the envelope. By comparing interferometer and single-dish observations at 1.3mm, Keene and Masson (1990) modelled the L1551/IRS5 source as an optically thick disk of size $\sim$ 45 A.U. surrounded by an extended, spherical

[1] L1551NE is also inferred to possess an outflow because of its characteristic cometary reflection nebula (Draper et al. 1985), its possible association with the L1551 W outflow (Moriarty-Schieven & Wannier 199]; Pound & Bally 1991), and from CO J=3-2 spectra (G. Moriarty-Schieven, unpublished). Its CO properties used in this work are derived from the latter.

[2] The James Clerk Maxwell Telescope is operated by the Royal Observatory Edinburgh on behalf of the Science and Engineering Research Council of the United Kingdom, the Netherlands Organization for Scientific Research, and the National Research Council of Canada.

envelope, Using their model as a basis for an estimate, as much as 15-2570 of the $800\mu m$ emission and 30-40'%0 of the $1100\mu m$ emission originates from the disk. Thus most of the emission arises from the envelope, but a significant fraction, especially at 11 00pm, arises from the disk.

4. RESULTS

4.1. Outflow Activity

There appears to be a good correlation (Fig, 1) between the $800\mu m$ flux density (F_{800}), and outflow activity as indicated by our earlier CO observations (Paper 1). In Paper Iwe showed that a large fraction, 75-80%, of the observed sources possesses a molecular outflow (Table 1, Column 8), and we showed that the quantity $\int T_a^* dv * (\Delta V_{av})^3$ is roughly proportional to the mechanical luminosity of the outflow (Leo), disregarding certain effects of temperature, outflow inclination, and optical depth. Fig. 1 shows a clear correlation, with $L_{CO} \sim F_{800}^{1.9\pm0.5}$ (with correlation coefficient $R = 0.79$).

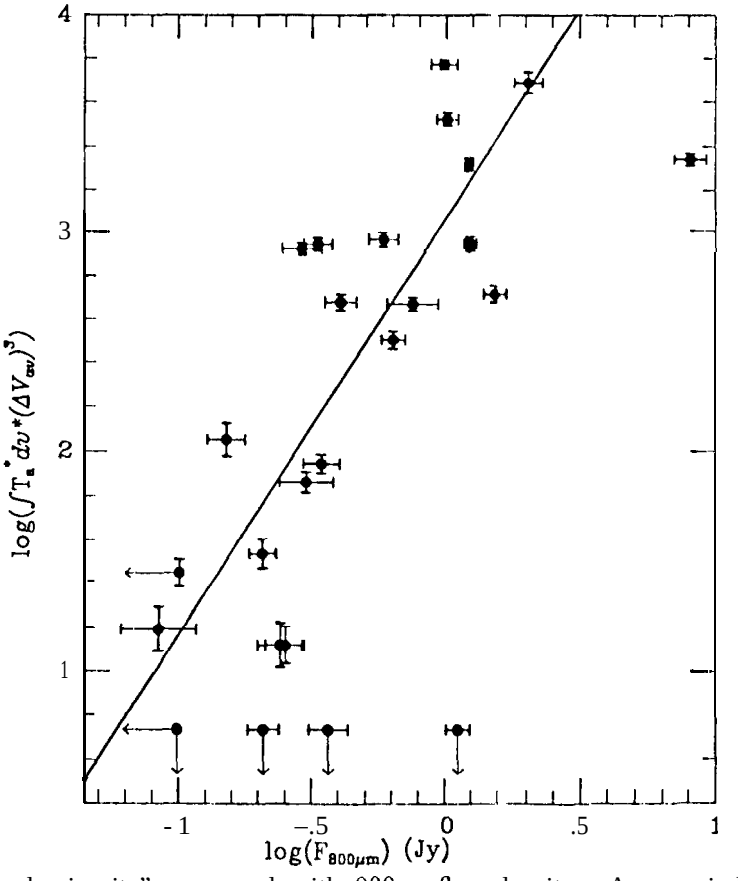

Fig. 1 .— "Outflow luminosity" compared with $800\mu m$ flux density. Arrows indicate upper limits. The diagonal line represents the best fit, which has a slow of 1.9+ 0.5,

It can also be seen that sources possessing outflows exhibit a wide range of flux densities at both 800 and 1100~im. This apparently contradicts the findings of Cabrit and André (1991), who found a significant

dichotomy in 1300pm flux density between sources possessing molecular outflows, and similar sources without outflows. Their apparent cutoff flux density of 0.25 J y at $1300\mu m$, below which no outflows were seen, suggested that a minimum disk (or envelope) mass was necessary to generate an outflow. Assuming a shallow λ^{-1} spectrum, this cutoff would correspond to flux densities of 0.295 J y and 0.406 J y at $1100\mu m$ and *800pm* respectively, whereas we have detected outflows towards sources whose $800\mu m$ flux density is <0.1 J y. We thus see no evidence for such a cutoff. Our different findings may reflect improved outflow search methods (Paper I), rather than different types of sources.

What does the correlation in Fig. 1 mean? One possibility is that the F_{800} is governed by the luminosity of the source. In Fig. 2 we compare F_{800} with the IRAS-derived far-infrared luminosity of the sources, and again find a good correlation with $L_{IR} \sim F_{800}^{1.2\pm0.3}$ (with correlation coefficient $R = 0.78$). 'I'his implies $L_{CO} \sim L_{IR}^{1.0\pm0.4}$. Cabrit and Bertout (1992) have found a very striking correlation between the bolometric luminosity of the source and its outflow luminosity in a study of known outflow sources, and found $L_{co} \sim L_{bol}^{0.8\pm0.08}$ (i.e. within 2a).

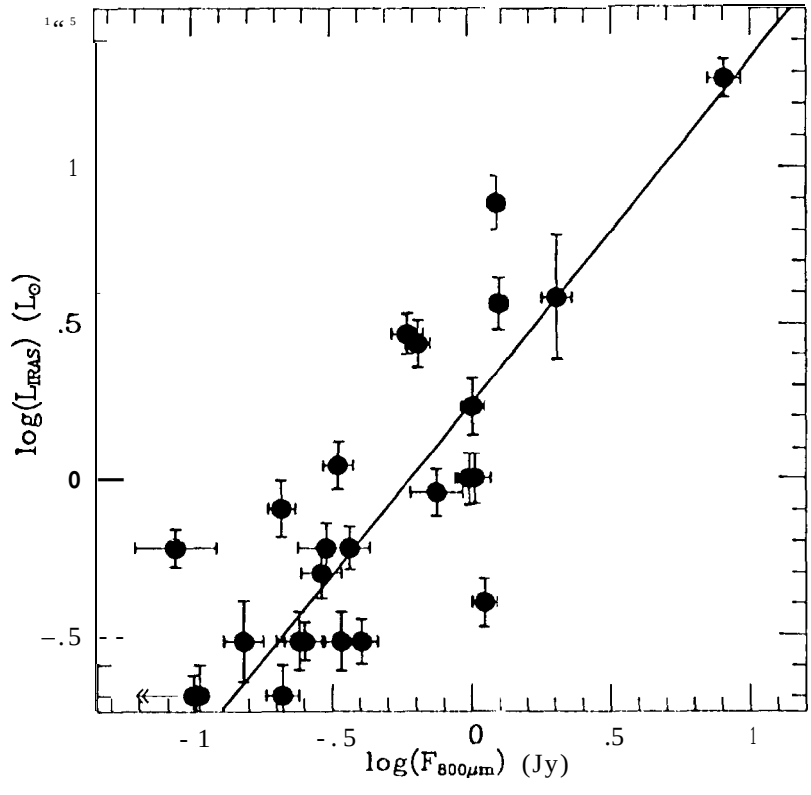

Fig. 2.— Far-infrared luminosity compared with $800\mu m$ *flux* density. Arrows indicate upper limits. The diagonal line represents the best fit, with slope 1.2 ± 0.3.

Another possibility is that outflow luminosity is correlated with the mass of the envelope/disk. Since the envelope is optically thin at $800\mu m$, the sub-millimeter emission is tracing the dust in the envelope/disk, and we can derive an estimate of its mass. From Hildebrand (1983), the mass of the (assumed isothermal)

envelope/disk can be written

$$M_{env} = \frac{F_\nu D^2}{B_\nu(T_d)} \left[\frac{4}{3}\frac{a\rho}{Q}\right] \left(\frac{M_g}{M_d}\right) \quad (1)$$

where F_ν is the flux density, D is the distance, $B_\nu(T)$ is the Plank function, a and ρ are the dust grain radius and density, (M_g/M_d) is the gas to dust mass ratio, and Q is the efficiency of emissivity of the dust. The ratio (M_g/M_d) is unknown in the dense circumprotostellar environment, and may indeed be variable from source to source. The emissivity efficiency Q is also highly uncertain, and published estimates range over a factor >30 (Draine 1989). Assuming these values are constant for all of our sources, the envelope/disk mass can be written

$$M_{env} \propto (e^{\frac{18.2}{T_d}} - 1) * F_{800}. \quad (2)$$

The dust temperature T_d was derived by fitting all available millimeter, sub-millimeter, and far-infrared observations (from this work and the *IRAS* point source catalogue, plus Barsony & Chandler (1993); Ohashi et al. (1991); Beckwith et al, (1990); Adams, Emerson & Fuller (1990); Weintraub, Sandell & Duncan (1989); Phillips et al. (1982); and Keene & Masson (1990)), using a non-linear least squares fit, to the function

$$F_\nu = \Omega B_\nu(T_d)(1 - e^{(\frac{\lambda}{\lambda_o})^{-\beta}}) \quad (3)$$

where Ω is the source solid angle, and λ_o the wavelength at which the optical depth is unity. The emission at 12 and 25μm was ignored in the fit because at such wavelengths the bulk of the emission comes from higher temperature material. Ω, T_d and λ_o were set as free parameters, and β was constrained to β = 1. Unfortunately because of the few data points for many sources, the solutions were not unique, and depending on the initial guesses the values for Ω and λ_o could vary by a factor of a few. The derived values for the dust temperature, however, generally varied by only a few Kelvin depending on the initial guess, since its value depends mainly on the 60-100μm flux densities. The temperatures used are the "average" values from several fits. (It should be noted that this dust temperature may not be characteristic of that of the 800μm emitting dust, and thus may represent an upper limit to the envelope dust temperature).

Armed with 800μm flux densities and estimates for the dust temperature (Table 2), we can estimate the disk/envelope mass. In Table 2 we have listed absolute values for mass, for which we have assumed a source distance of 150pc, a gas to dust mass ratio M_g/M_d = 100, and a dust emissivity from Hildebrand (1983) of $\left[\frac{4}{3}\frac{a\rho}{Q}\right] = 0.1\left(\frac{\lambda}{250\mu m}\right)^{\beta}$ g cm^{-2} using $\beta = 1$ (Beckwith et al. 1990). The values for mass range from 1.5 x 10^{-3} to 1.4 x $10^{-1} M_\odot$, but because we are mainly interested in the correlation of mass with luminosity, the absolute values are not critical. Comparing the estimated mass with the outflow luminosity and with far-infrared luminosity (Fig. 3), we again find a good correlation, $L_{CO} \sim M_{env}^{2.1 \pm 0.7}$ and $L_{IR} \sim M_{env}^{0.82 \pm 0.20}$ (with correlation coefficients R = 0.70 and 0.68 respectively). Thus the mass of the circumstellar disk/envelope may be linked to the generation of outflows and, perhaps, accretion,

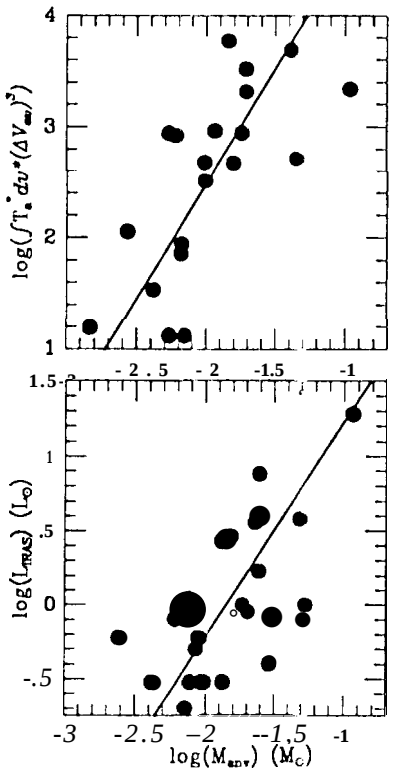

Fig. *3.*— (upper) Comparison of "outflow luminosity" with an estimate for the mass of the circumstellar envelope. The diagonal represents the best fit, with slope 2.13 0.7. (lower) Comparison of IRAS luminosity with mass of the envelope. The line of best fit here has slope 1.3 $\pm$ 0.5.

4.2. The Spectral Energy Distribution & Disk/Envelope Evolution

As the protostar evolves, one expects changes in the properties of the disk/envelope. The envelope presumably shrinks as it accretes onto the circumstellar disk, while the disk should become more optically thick as it builds up mass. One might also expect that the dust properties themselves will change, since the standard model for planet formation starts with the growth of dust particles. 130th effects can be expected to affect the spectral energy distribution (SED) of the disk/envelope at long wavelengths. For example, the more optically thick disk in the evolved object may tend to dominate the SED at longer wavelengths, making the spectral index shallower. Also, in a denser disk environment, dust particles should be growing "fluffier", changing the dust emissivity law β. Spherical dielectric grains have $\beta = 2$ (Draine & Lee 1984), while '(fluffy", fractal particles may have $\beta \lesssim 1$ (Wright 1987).

At millimeter/sub-millimeter wavelengths, the SED of warm dust can be expressed as a power law, i.e. $F_\nu \propto \lambda^{-\alpha}$, where α is the spectral index. The value of α is easily derived from our data (Table 2). To test for evolutionary effects, we wish to compare our values of the spectral index α with similarly derived values of a sample of more evolved objects. Beckwith & Sargent (1991) have observed the sub-millimeter emission from a selection of T Tauri stars, primarily in the Taurus complex. From these they derived the dust emissivity law β, which is related to α by $\alpha = \beta + 2$ (from equation 3). These sources *were chosen* for comparison with ours because of their similarity in luminosity (the mean luminosity for both sets of objects is $\sim 2 L_\odot$).

We note that several of the sources in Beckwith & Sargent's list satisfy our primary selection criterion, which is that their colour temperatures indicate them to be "cold" (i.e. $log[F_{25\mu m}/F_{60\mu m}] < -0.25$). We thus compare the values of α from the 25 "cold" sources (from both lists, using our values of α when available) with those of the 16 "warm" sources (i.e. $log[F_{25\mu m}/F_{60\mu m}] > -0.25$). We grouped the "warm" and "cold" sources each into $\Delta\alpha \sim 0.5$ wide bins (and normalized the number of sources in each "warm" bin to sum to 25), and display the histogram of these distributions in Fig. 4 (top panel).

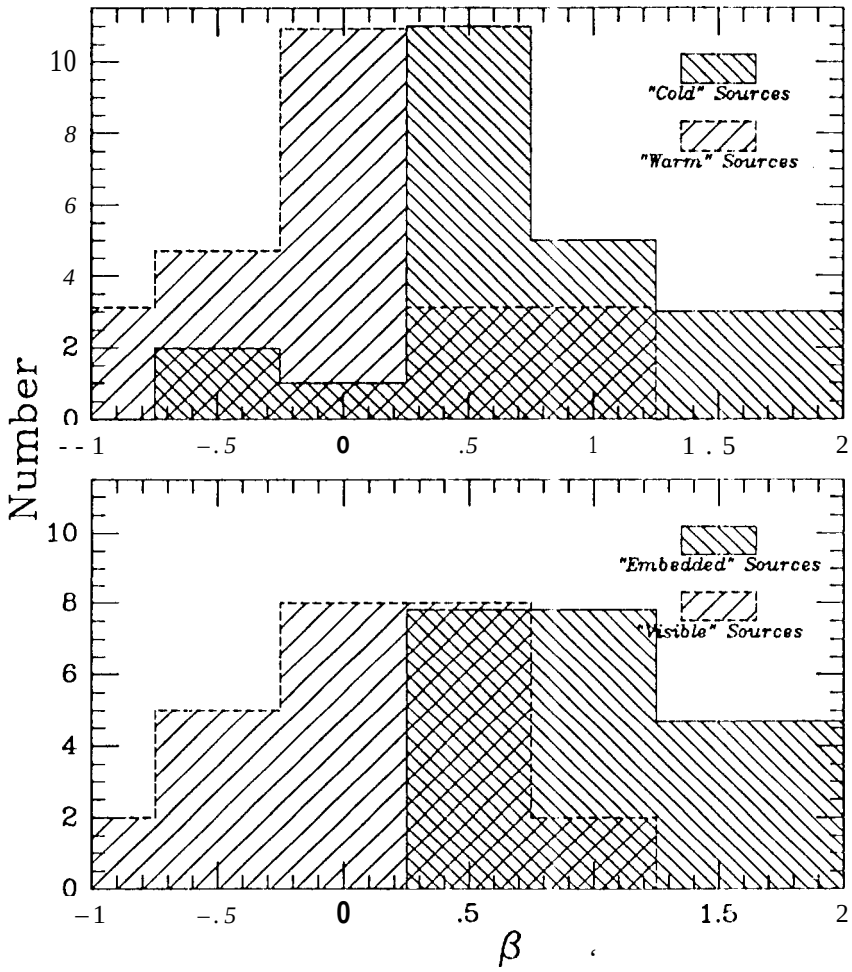

Fig. 4.— (upper) Histogram comparing the distributions of dust emissivity indices (β) for "cold" young stellar objects ($log[F_{25\mu m}/F_{60\mu m}] < -0.25$) and "warm" objects ($log[F_{25\mu m}/F_{60\mu m}] > -0.25$). Data were taken from this work and from Beckwith & Sargent (199]). (lower) Same as ahove except that sources are grouped according to whether they are "embedded" or optically "visible". For both histograms, the numbers for each group have been normalized to sum to 25.

This figure shows a significant difference in the distributions of α for the two samples. "Warm" sources have a distribution skewed toward smaller values of α, while "cold" sources are skewed toward higher values of α. If instead we group our objects and those of Beckwith & Sargent into whether the source is optically "visible" or "embedded" (25 "visible", 16 "embedded"), we get an even greater difference in the distribution

of α (Fig. 4, lower panel). (For the five objects which have been observed both by us and by Beckwith & Sargent, we note that our values of α are not significantly different from those of Beckwith & Sargent, but our values tend to be smaller.)

It must be noted that there is considerable error in our values of α, which could weaken the apparent differences in the two data sets. However, we can quantify this uncertainty by applying the Kolmogorov-Smirnov (K-S) and χ^2 statistical tests, incorporating our error estimates. These tests estimate the probability that the two data sets are drawn from the same sample, the former for continuous data and the latter for binned data, Measurement error was incorporated by running a Monte Carlo simulation of the two datasets. After 100000 trials comparing the spectral indices of visible versus embedded objects, the K-S test found that 99% of the trials had a probability of < 4% that the two datasets were the same, while the χ^2 test showed that 95% of the trials had a probability of < 9% that the datasets were the same. Thus we have a very high confidence that T Tauri stars have significantly shallower spectral indices than younger, embedded objects.

One further effect may affect the derived SED. Because the apertures used to mea-sure the flux densities are larger at the longer wavelengths, the derived SED may be artificially skewed to low numbers if the source is extended. Although the apertures we used were very similar in diameter (16.8" and 18.5" at 800 and 1100μm respectively) the ones used by Sargent and Beckwith were somewhat more discrepant (17" and 22"). However, as noted above, for the sources that were observed by both groups our SEDS tended to be flatter, implying that the aperture diameter had a minor effect, if any, on the SED. Moreover, as noted below, André & Montemerle (1 994) found that a larger fraction of the embedded objects were resolved by a 12" beam than the visible sources. This implies that the S1 :Ds of embedded objects should be flattened more by beam-size effects than visible objects. Yet this is opposite the observed trend.

Figure 4 shows that visible objects have a much shallower SED than embedded objects, and to a lesser extent, the same is true of "warm" disk/envelopes compared to "cold" disk/envelopes. Even those cold objects which are visible tend to have shallower SEDS than cold embedded objects. These effects could be due to the contraction of the envelope, to the evolution of dust grains, or to both effects.

Evidence has been presented for the contraction of the circumstellar envelope by Ohashi et al. (1991), who compared interferometric observations of CS J=2-1 and 98 GHz (~3mm) continuum emission from six "embedded" and five "visible" young stellar objects in Taurus. They found that most of the embedded objects were detected in CS but few in continuum emission, while the opposite was true of the visible objects, From this they concluded that the distribution of circumstellar material was more concentrated toward the center for the more evolved objects than for the visible objects.

Ten of their eleven objects were also observed by us or by Beckwith & Sargent (1991). The embedded and visible objects have a similar range of 800μm ffux densities, but the embedded sources have steeper spectral indices. If we extrapolate the 800 and 1100μm emission down to 3mm, the expected emission is close to that observed (or upper limits) by Ohashi et al. This would suggest that spectral indices continue to be steeper for embedded sources compared to visible sources, even into millimeter wavelengths,

André & Montmerle (1 994) have found more direct evidence for the contraction of the circumstellar envelope. They presented 1 .3mm continuum observations of more than 100 young stellar objects in the ρ Ophiuchus complex, and found that a much larger fraction of embedded (Class 1) objects were resolved at 12" than visible objects. From this and other evidence, they conclude that the differences between embedded and visible young stellar objects are mainly due to differences in the spatial distribution of circumstellar dust.

Finally, we note that wc see no difference in the distribution of masses between embedded and visible objects if we assume, in spite of the difference of the spectral indices, t hat the grain emissivity is the same for both these samples at $800\mu m$. This could imply that most of the circumstellar material near the embedded sources eventually is accreted onto the circumstellar disk,

4.3. sources without Outflows

Because of the good correlation between $800\mu m$ flux density and far-i nfrared and outflow mechanical luminosities (see sec. 4.1 .), the wide range of flux densities of those sources without outflows is puzzling. One of these, GG 'I'au (04296+1725), is especially peculiar in that it has an anomalously large sub-millimeter flux density (Table 1) compared to its $100\mu m$ flux density of 5.2 Jy.

There are, however, several things that these non-outflow sources appear to have in common. Most notably, these four objects, all optically visible, have the weakest ^{12}CO J=3-2 emission associated with them of all the objects in this survey (Paper 1). Indeed, 04 154+ 1755 had no CO detected toward it, and the rest had only weak emission ($0.1\ K < T_a^*(peak) < 0.6K$). Skrutskie et al (1993) reported detecting no extended ^{12}CO J=1-0 emission toward GG Tau (04296+ 1 725)exceptin its immediate vicinity. Thus even if these objects have some sort of outflow activity (Haro 6-13 posse.sscs an optical jet (Strom et al 1986)), there may be too little ambient CO for molecular outflows to be seen associated with them.

Another feature that these objects appear to have in common is a ver y shallow spectral index in the sub-millimeter (except for 04154+1755, which was not detected). Indeed, GG Tau, Haro 6-13, and HK Tau (04288+24 17) have the smallest values of& (Table 2) of all of t he sources, suggesting perhaps that they have the most evolved envelopes (see sec. 4.2.).

5. SUMMARY

We have obtained $800\mu m$ and 1100pnt photometry of a complete, flux-limited, IRA S-selected sample of objects in Taurus, whose infrared and molecular properties indicate them to be low-mass protostars which are younger than T Tauri stars. All but two were detected at $800\mu m$, and all but four at $1100\mu m$.

We find a good correlation between the mm/sub-mm flux density and the energetic of the molecular outflow, with $L_{co} \sim F_{800}^{1.0\pm0.5}$. We also find that the $800\mu m$ flux density correlates with the IRAS-derived luminosity of the protostar, with $L_{IRAS} \sim F_{800}^{1.2\pm0.3}$. This implies that outflow activity is linked to the luminosity of the protostar, as found by Cabrit & Bertout (1992).

Using a simple greybody model, we used all available far-infrared through millimeter data to estimate the temperature and hence derive an estimate for the mass of the emitting region. We find that the disk/envelope ***mass*** may be well correlated with outflow activity, such that $L_{CO} \sim M_{env}^{2.1\pm0.7}$ We also find that $L_{IRAS} \sim M_{env}^{1.3\pm0.5}$. This suggests that the mass of the circumstellar envelope and disk may be linked to outflow activity and the far-infrared luminosity. However, in contrast to the results of Cabrit & André, we see no evidence for a lower limit to the disk/envelope mass which can produce outflows.

We have found evidence that the spectral index (α) is significantly steeper in the sub-millimeter for younger, colder, embedded young stellar objects than for more evolved, optically visible objects, and there are indications that these indices continue to be steeper into millimeter wavelengths. This would suggest

that (a) dust grains are evolving and changing the emissivity law, and/or (h) the temperature/density distribution of the circumstellar envelope/disk changes, tending to "flatten" the spectal energy distribution at millimeter and sub-millimeter wavelengths. We see no differences, however, in the distribution of masses between embedded and visible sources, implying that most of the circumstellar material near embedded sources is eventually accreted onto the circumstellar disk.

Finally, we note that the sources in our sample which possess no molecular outflow, have both the least amount of ambient CO associated with them and the shallowest spectal indices (α). This suggests that there may be insufficient ambient C() to see a molecular outflow despite the presence of at least one optical jet, and also suggests that these sources may have the most evolved circumstellar envelopes of the sample.

We wish to thank 11. Butner for helpful discussions, and our anonymous referee for useful suggestions. G. M.-S. is supported by a research associateship from the National Research Council of Canada. This work was carried out, in part, by the Jet Propulsion Laboratory, California Institute of Technology, under a contract with the National Aeronautics and Space Administrate ion. The Caltech Submillimeter Observatory is supported by NSF Grant 90-15755.

REFERENCES

Adarns F. C., Emerson J. P., & Fuller, G. A. 1990, ApJ, 357, 606

Adams, F. C., Lada, C. J., & Shu, F.H. 1987, ApJ, 312, 788

André, P., & Montmerle, 1'. 1994, ApJ, in press

Barsony, M., & Chandler, C. J. 1993, ApJ, 406, L71

Beckwith, S. V. W., Sargent, A. l., Chini, R. S., & Gusten, R. 1990, AJ, 99, 924

Beckwith, S. V. W., & Sargent, A. I. 1991, ApJ, 381, 250

Beichman, C. A., Myers, P. C., Emerson, J. P., Harris, S., Mathieu, R., Benson, P. J., & Jennings, R. E. 1986, ApJ, 307, 337

Cabrit, S., & André, P. 1991, ApJ, 379, L25

Cabrit, S., & Bertout, C. 1992, A&A, 261, 274

Draine, B. T. 1989, *Proc. of 22nd ESLAB Symposium on Infrared Spectroscopy in Astronomy*, ed. B. H. Kaldeich (ESA Publications, Noordewijk)

Draine, B. T., & Lee, II. M. 1984, ApJ, 285, 89

Draper, P. W., Warren-Smith, R. F., & Scarrot, S. M. 1985, h! NRAS, 216, 7p

Duncan, W. D., Robson, E. 1., Ade, P. A. R., Griffin, M. J., & Sandell, G. 1990, MNRAS, 243, 126

Emerson, J. P., Harris, S., Jennings, R. E., Beichman, C. A., Buad, B., Beintema, D. A., Marsden, P. L., & Wesselius, P. R. 1984, ApJ, 278, L49

Hartmann, L., & Kenyon, S. J. 1985, ApJ, 299, 462

Hildebrand, R. H. 1983, QJRAS, 24, 267

Keene, J., & Masson, C. R. 1990, ApJ, 355, 635

Matthews, H.E. 1993, *"The James Clerk Maxwell Telescope: A Guide for the Prespective User"* (Joint Astronomy Centre Technical Report)

Moriarty-Schieven, G. 11., & Wannier, P. G. 1991, ApJ, 373, L23

Moriarty -Schieven, G. 11,, Wannier, P. G., Tamura, M., & Keene, J. 1992, ApJ400, 260 (Paper 1)

Myers, P. C., Fuller, G. A., Mathieu, R.D., Beichman, C. A., Benson, P. J., & Schild, R. E. 1987, ApJ, 319, 340

Ohashi, N., Kawabe, R., Hayashi, M., & Ishiguro, M. 1991, AJ, 102, 2054

Phillips, J. P., White, G. J., Ade, P. A. R., Cunningham, C. J., Richardson, K. J., Robson, E. I., & Watt, G. D. 1982, A&A, 116, 130

Pound, M. W., & Bally, J. 1991, ApJ, 383, 705

Shu, F.H., Adams, F. C., & Lizano, S. 1987, ARA&A, 2.5, 23

Skrutskie, M. F., Snell, R.L., Strom, K. M., Strom, S. E., Edwards, S., Fukui, Y., Mizuno, A., Hayashi, M., & Ohashi, N. 1993, ApJ, 409, 422

Strom, S. E., Strom, K. H., Wollf, S. C., Morgan, J., & Wenz, M. 1986, ApJS, 62, 39

Tamura, M., Gatley, I., Wailer, W., & Werner, M. W. 1991, ApJ, 374, 1.25

Tamura, M., & Sate, S. 1989, AJ, 98, 1368

Weintraub, D. A., Sandell, G., & Duncan, W. D. 1989, ApJ, 340, 1,69

Wright, E. L. 1987, ApJ, 320, 818

Table 1. Sources and Flux Densities

IRAS	ID	R.A.	Dec.	~1100;11), Jy	$F_{800\mu m}$ Jy	L_{IRAS} $L_\odot$	CO?	Ref
1	2	3	4	5	6	7	8	9
04016+2610	L1489IRS	$4^h01^m40\overset{s}{.}6$	26°10'49"	0.180 ± 0.021	0.582 ± 0.079	2.9	Y	1
04108+2803		4 1049.3	280357	<0.1	0.085 ± 0.033	0.6	?	1
04113+2758		411 20.8	275833	0.461 ± 0.053	0.98 ± 0.12	1.0	Y	1
04154+1755		4 15 28.3	175526	<0.1	<0.1	0.2	N	1
04169+2702		4 16 53.8	270252	0.281 ± 0.053	0.75 ± 0.18	0.9	Y	1
04181+2655		4 18 05.5	*265437*	0.044 ± 0.026	0.152 ± 0.027	0.3	?	1
04190+1924	1' Tau	4 1904.2	*192505*	0.579 ± *0.027*	1.216 ± 0.044	7.6	Y	2
04191+1523		4 19 09.6	152320	0.179 ± 0.027	0.404 ± 0.056	0.3	Y	1
04239+2436		42354.5	243654	0.114 ± 0.021	0.333 ± 0.043	1.1	Y	1
04240+2559	DG Tau	42401.0	255936	0.532 ± 0.048	1.233 ± 0.066	3.6	Y	2
04248+2612	HH31 IRS	42452.7	261242	0.099 ± 0.015	0.252 ± 0.046	0.3	Y	1
04287+1801	L1551IRS5	42840.2	180141	2.77 ± 0.30	8.05 ± 1.23	19.	Y	1
04288+2417	HK Tau	42848.9	241756	0.110 ± 0.020	0.210 ± 0.030	0.2	N	3
	L1551NE	42850.5	180210	0.836 ± 0.076	2.03 ± 0,27	3.8	Y	1,4
04292+2422	H6-13	42913.6	242243	0.223 ± 0.022	0.3663, 0.066	0.6	N	1
04295+2251	L1536IRS	42932.2	2251 11	0.094 ± 0.018	0.2415, 0.050	0.3	Y	1
04296+1725	GG Tau	42937.1	172522	0.74 ± 0.12	1.113, 0.12	0.4	N	1
04302+2247		43016.4	224704	0.149 ± 0.019	0.3423:0.057	0.3	Y	1
04325+2402		43233.5	240215	0.074 ± 0.015	0.3013:0.079	0.6	Y	1
04328+2248	HP Tau	43252.9	224818	<0.1	0.2083:0.025	0.8	Y	2,3
04361+2547		43609.8	254730	0.188 ± 0.027	0.634 ± 0.067	2.7	Y	1
04365+2535		43631.2	253556	0.438 ± 0.038	1.01 ± 0.10	1.7	Y	1
04368+2557	1.1.527	43649.8	255721	0.482 ± 0.037	1.523:0.15	1.0	Y	1
04381+2540		43808.5	254053	0.116 ± 0.013	0.289 ± 0.053	0.5	Y	1
04390+2517	LkHα 332	43904."	251733	<0.1	<0.1	0.2	Y	1

References. — (1) This work; ('2) Weintraub, Sandell & Duncan (1989); (3) Adams, Emerson & Fuller (1990); (4) IRAS flux densities from Emerson et al. (1 984).

Table 2. Derived Properties

IRAS	ID	α	T_d K	M_{env} $M_\odot$
04016+2610	L1489IRS	3.65± 0.56	43	0.012
04108+2803		. .	48	0.0015
04113+2758		2.34 ± 0.52	55	0.015
04154+1755		. .	...	...
04169+2702		3.04 ± 0.96	40	0.016
04181+2655		3.85 ± 1.20	47	0.0027
04190+1924	T Tau	2.31 ± 0.18	51	0.020
04191+1523		2.53 ± 0.64	36	0.010
04239+2436		3.3350.70	51	0.0054
04240+2559	DG Tau	2.61 i 0.32	55	0.018
04248+2612	HH31 IRS	2.90 ± 0.74	33	0.0070
04287+1801	L1551IRS5	3.31 ±0.57	47	0.14
04288+2417	HK Tau	2.01 ± 0.72	37	0.0050
	L1551NE	2.76 ± 0.39	42	0.042
04292+2422	Haro 6-13	1.54 ± 0.62	48	0.0064
04295+2251	L1536IRS	2.93 ± 0.89	39	0.0054
04296+1725	GG Tau	1.28 ± 0.59	40	0.024
04302+2247		2.58 ± 0.65	44	0.0066
04325+2402		4.36 ± 1.04	40	0.0065
04328+2248	HP Tau	> 1.88	43	0.0041
04361+2547		3.78 ± 0.55	53	0.0098
04365+2535		2.60 ± 0.41	44	0.020
04368+2557	L1527	2.34 ±0.49	31	0.046
04381+2540		2.84 ±0.53	41	0.0061
04390+2517	LkHα 332	...	...	...